OPTIMIZATION OF PULSE WIDTH FOR ELECTRIC TDR FOR FAULT POINT LOCALIZATION OF POWER FEEDING LINES OF SUBMARINE CABLES

Junichi Kojima (KDDI R&D Laboratories Inc.)

Email: kojima@kddilabs.jp

KDDI R&D Laboratories Inc, 2-1-15 Ohara, Kamifukuoka-shi, Saitama, Japan

Abstract: The location of the failure point of the power feeding line of a submarine cable can be measured using electric time domain reflectometry (TDR). In TDR, the round-trip time of an electric pulse is measured. However, as the frequency dispersion and attenuation of the electric signals propagating in the power feeding lines are large, it is not easy to accurately calculate the fault point from the round trip time. In this paper, we discuss optimum pulse width from the viewpoint of attenuation of the pulse. The frequency and time domain analysis of the power feeding line of the LW and SAM cables are used to obtain the optimum pulse width.

1 INTRODUCTION

Most causes of submarine cable failure are short-circuiting of power feeding lines to the seawater. The location of failures can be measured with high accuracy using an optical time domain reflector (OTDR). But when optical fibres are unbroken, the fault position can only be located from the landing stations with an electric time domain reflector (TDR), DC resistance measurement or capacitance measurement method.

The round-trip propagation time of an electric signal is measured by TDR. Figure 1 shows a typical configuration of the TDR measurement. For example, Figs. 2 and 3 show the TDR result of the actual cable that had a shunt fault 5.5km away from the landing station. These figures show that the pulse propagation time changes by the width of the pulse. This means that the frequency dispersion of the transmission line is large. Therefore, it is important to know the propagation velocity corresponding to the pulse width in order to calculate the distance to the fault point accurately from the round-trip propagation time. In addition, because attenuation of the echo signal increases as the pulse width shortens, the selection of the pulse width for TDR is also an important factor for accurate measurement.

Therefore, we analyzed the propagation characteristic of the power feed line of single armored (SAM) cables and light weight (LW) cables. In this paper, we propose a method for selecting the optimum pulse width corresponding to the distance using the results of numerical time domain simulation of the TDR.

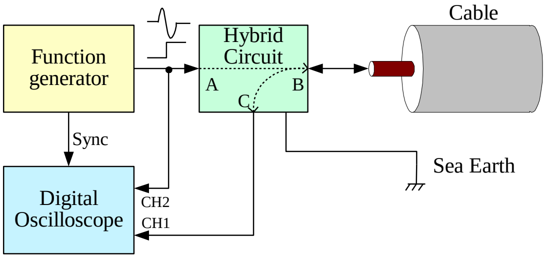

Figure 1: Block diagram of TDR

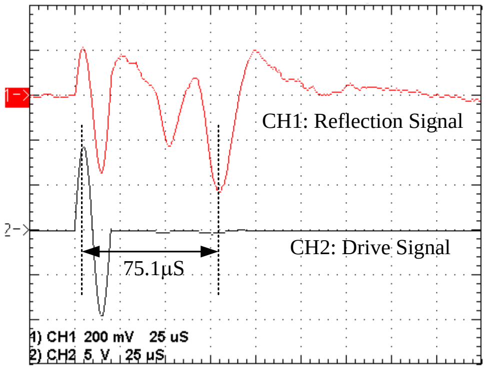

Figure 2: Result of TDR using a sinusoidal pulse [4] (PW=20μS)

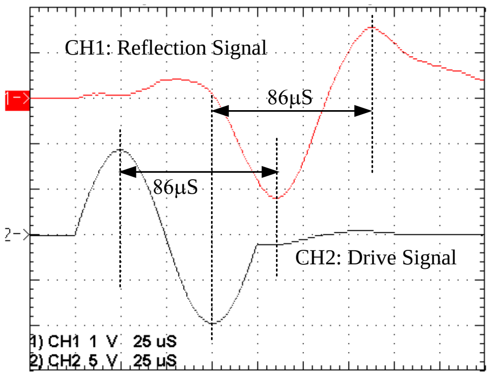

Figure 3: Result of TDR using a sinusoidal pulse [4] (PW=100μS)

2 ANALYSIS OF PROPAGATION CHARACTERISTIC OF POWER FEEDING LINE

2.1 Numerical analysis of LW cable

Figure 4 shows the cross section of the LW cable. The inner conductor is composed of an iron tube, steel wires and a copper tube. The surrounding seawater is the outer conductor in which the return current flows.

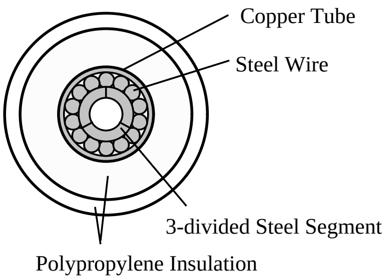

Figure 4: Cross-section view of LW cable

The electric current flowing in the LW cable can be expressed as follows. The details are shown in the reference [1].

$$I = I_0 \exp(j\omega t - jk_z z) \tag{1}$$

Where,

$$k_z = \sqrt{k_2{}^2 - k_{r2}{}^2} \tag{2}$$

$$k_{r2} = \frac{k_2{}^2}{\sqrt{-j\mu\omega \ln(a_2/a_1)}} \bullet \left(\frac{J_0(k_{r1}a_1)}{\sqrt{\sigma_1 a_1} J_1(k_{r1}a_1)} - \frac{H_0^{(2)}(k_{r5}a_2)}{\sqrt{\sigma_5 a_2} H_1^{(2)}(k_{r5}a_2)} \right) \tag{3}$$

$$k_{r1} = \sqrt{k_1{}^2 - k_z{}^2}, k_{r1} = \sqrt{k_1{}^2 - k_z{}^2}, \quad k_1 = \sqrt{\mu\varepsilon\omega^2 - j\mu\sigma_1\omega} \tag{4}$$

$$k_{r1} = \sqrt{k_1{}^2 - k_z{}^2}, k_{r1} = \sqrt{k_1{}^2 - k_z{}^2}, \quad k_1 = \sqrt{\mu\varepsilon\omega^2 - j\mu\sigma_1\omega} \tag{5}$$

$$k_2 = \sqrt{\mu\varepsilon\omega^2}, k_1 = \sqrt{\mu\varepsilon\omega^2 - j\mu\sigma_5\omega} \tag{6}$$

a, μ, ε, σ denote radius, permeability, dielectric constant, and conductivity, respectively. Subscripts 1, 2, and 5 denote the inner conductor, the dielectric and seawater, respectively.

The frequency characteristics of the loss, phase velocity, and group velocity are calculated from the propagation constant $k_{z.}$ The results are shown in Fig. 5. This figure shows that the propagation velocity of the LW cable is considerably slow compared with that of the coaxial cable (typically 2×10^8m/s).

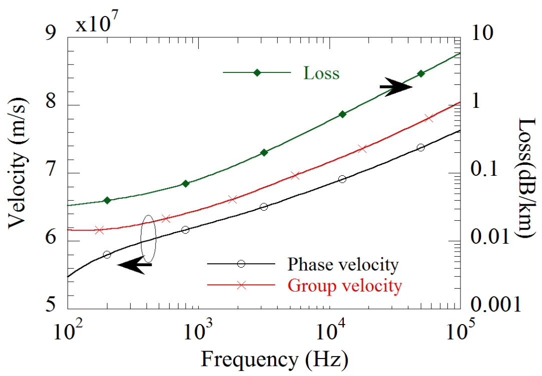

Figure 5: Frequency characteristics of the phase, the group velocity and the loss of the LW cable

The time-domain waveform can be expressed by the following Fourier Transform.

$$v_O(t) = \int_{-\infty}^{\infty} V_I(\omega)\exp(jwt - jk_z(w)z)d\omega$$

Where $V_I(\omega)$ is the Fourier Transform of the input signal $v_i(t)$.

Figure 6 shows an example of the numerical calculation result of the sinusoidal pulse response of TDR propagated in the LW cable. In this calculation, the pulse width of the input signal is 10µS, and the length of the cable is 1, 2, 5, and 10km. This figure shows that the reflected wave attenuates and expands as the length of the cable increases.

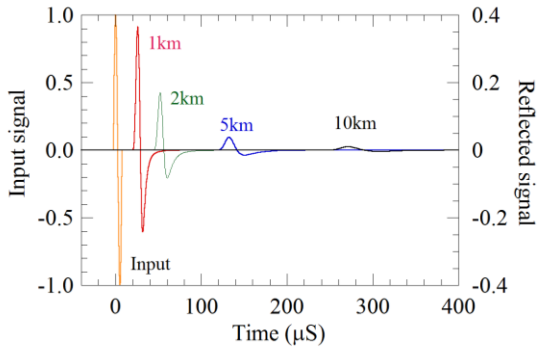

Figure 6: Simulation result of TDR (LW cable, pulse width=10µS)

2.2 Numerical analysis of SAM cable[3]

We also analyzed the transmission characteristics of an armored cable laid on the seabed using the technique described in the EMTP Theory Book. Figure 7 shows the simulation model of the armored cable. Because details of the analysis are described in reference [3], only the result is shown here.

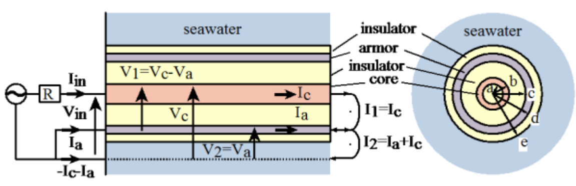

Figure 7: Simulation model of armored cable[3]

The correlations between I_1, V_1, I_2, and V2 in Fig. 7 are expressed by the following equation.

$$\begin{bmatrix} \gamma & 0 & Z_{11} & Z_{12} \\ 0 & \gamma & Z_{21} & Z_{22} \\ Y_{11} & 0 & \gamma & 0 \\ 0 & Y_{22} & 0 & \gamma \end{bmatrix} \begin{bmatrix} V_1 \\ V_2 \\ I_1 \\ I_2 \end{bmatrix} = 0 \qquad (7)$$

V_1 is voltage between the inner conductor and the armor wire, and V_2 is voltage between the armor wire and the seawater.

The propagation constant γ of the armored cable can be obtained from the following eigen equation:

$$\gamma^4 - \gamma^2\left(Y_{11}Z_{11} + Y_{22}Z_{22}\right) + Y_{11}Y_{22}\left(Z_{11}Z_{22} - Z_{12}^2\right) \quad (8)$$

Here, Z_{xx} and Y_{xx} are impedance and admittance calculated from the structure and material shown in Table I.

Radius of inner conductor	$4.44\text{x}10^{-3}$ m
Conductivity of inner conductor	$5.8\text{x}10^{-7}$ S/m
Relative permeability of inner conductor	1
Radius of insulator	$5.25\text{x}10^{-3}$ m
Conductivity of insulator	0 S/m
Relative permittivity of insulator	2.27
Relative permeability of insulator	1.0
Radius of armored wire layer	$11.8\text{x}10^{-3}$m
Conductivity of armored wire layer	$4.5\text{x}10^{6}$ S/m
Relative permeability of armored wire layer	90
Radius of seawater layer	$17.0\text{x}10^{-3}$ m
Conductivity of seawater layer	4.0 S/m
Relative permittivity of seawater layer	81.0
Relative permeability of seawater layer	1.0

Table 1: Parameters of SAM cable

The frequency characteristics of the loss, phase velocity, and group velocity can be calculated from the propagation constant γ. The results are shown in Fig. 8. This figure shows that the characteristics of the SAM cable differ considerably from those of the LW cable shown in Fig. 5.

Figure 9 shows an example of the numerical calculation result of the sinusoidal pulse response propagated in the

SAM cable. This figure shows the waveform changes of the reflected signal from the cable end with a length of 10km when the pulse width is changed. The pulse width of the reflected signal is expanded by the frequency dispersion.

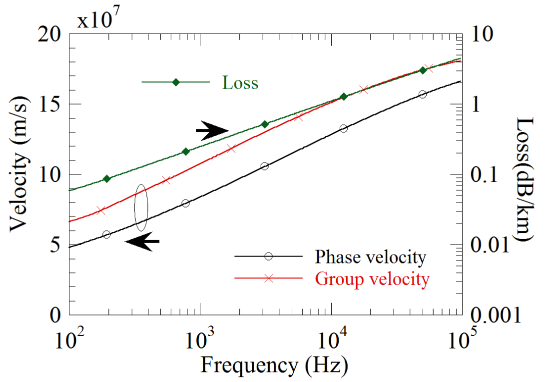

Figure 8: Frequency characteristics of the phase, the group velocity and the loss of the SAM cable

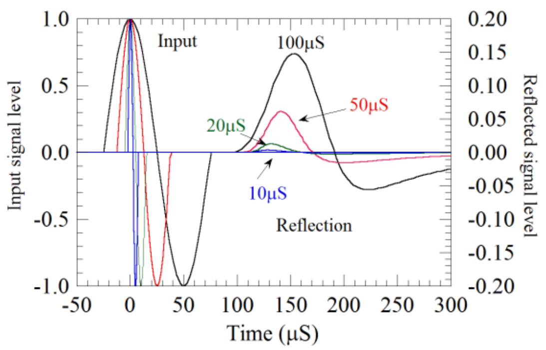

Figure 9: Simulation result of TDR (cable length=10km)

3 OPTIMIZATION OF PULSE WIDTH FOR TDR

In the actual measurement of TDR, the accuracy is limited by the signal-to-noise ratio of the reflection signal. For example, in the noisy environment, a permissible attenuation of the reflection pulse is limited. In this case, wide pulse is required to reduce the attenuation of the signal. But it also reduces the resolution of the distance to the fault point.

In order to obtain maximum resolution under the noise, we calculated the correlation between pulse width, loss and propagation distance using the simulation results of TDR. Figures 10 and 12 show the results of this calculation for the LW and SAM cable, respectively. Figures 11 and 13 also show the correlation between pulse propagation velocity, loss and distance.

TDR measurement is summarized as follows:

(1) Measure the rough distance using step pulse.

(2) Using Figs. 10 or 12, obtain the optimum pulse width of the sinusoidal pulse corresponding to the distance with the given attenuation. For example, if the distance is 10km and attenuation is 30dB, the optimum pulse width is 30µS from Fig. 12.

(3) Measure round trip time using this condition by TDR.

(4) Using Figs. 11 or 13, obtain the pulse propagation velocity, and multiply the result of (3), and calculate the correct distance to the fault point. For example, if the distance is 10km and attenuation is 30dB, the velocity is 14.7×10^7m/s based on Fig. 13.

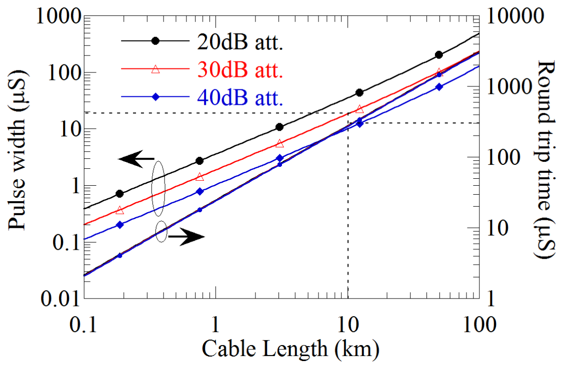

Figure 10: Sinusoidal pulse width vs. length of cable based on the attenuation of the reflection signal (LW cable)

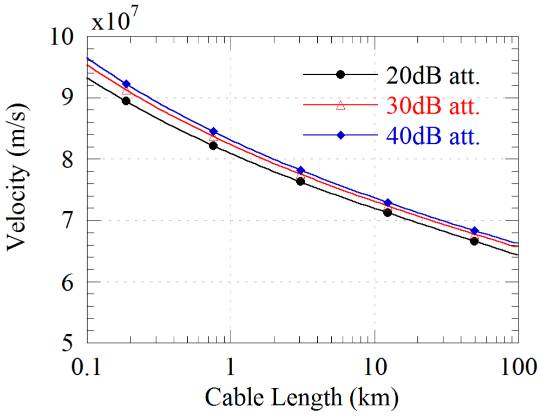

Figure 11: Pulse propagation velocity vs. cable length (LW cable)

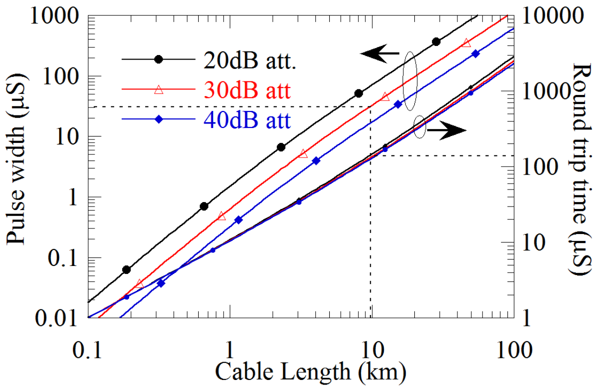

Figure 12: Sinusoidal pulse width vs. length of cable based on the attenuation of the reflection signal (SAM cable)

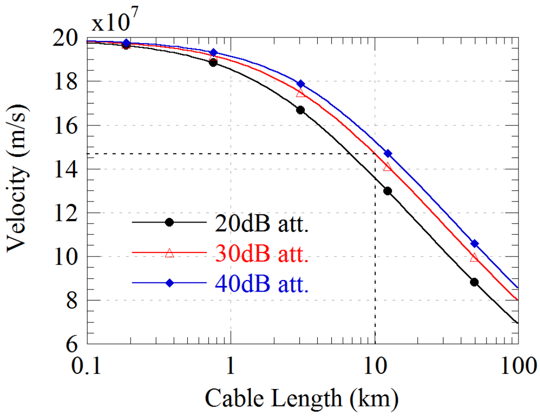

Figure 13: Pulse propagation velocity vs. cable length (SAM cable)

4 CONCLUSION

As techniques for locating the fault point in the power feeding line of an optical submarine cable, electric TDR is commonly used. It is necessary to know the pulse velocity propagating in the power feeding line in order to calculate the distance to the fault point.

In this paper, we proposed TDR measurement using an optimum sinusoidal pulse in order to increase the accuracy of the measurement.

5 REFERENCES

[1] K. Asakawa and J. Kojima, "Localization of fault point of optical underwater telecommunication cable with electric method," Proc. of SUBOPTIC'93, pp. 513-517, 1993.

[2] J. Kojima, S. Matsumoto and K. Asakawa, "Fault point localization of power feeding lines in optical submarine cables," Proc. OCEANS'08 MTS/IEEE Quebec, Sept. 2008.

[3] J. Kojima, S. Matsumoto, K. Asakawa, and T. Asami, "Fault Point Localization of Armored Optical Submarine Cables using Electric Time Domain Reflectometry and Frequency Domain Reflectometry", IEICE, Volume J93-B No.6, 2010

[4] J. Kojima, "Fault Point Localization of Power Feeding Lines in Optical Submarine Cables Using Electric Time Domain Reflectometry and Frequency Domain Reflectometry", SubOptic2010, 2010